Fifty Years of Wide Field Studies in the Southern Hemisphere
ASP Conference Series, Vol. 491
S. Points and A. Kunder, eds.

Age and Metallicity Analysis of the Small Magellanic Cloud from Star Clusters

M. C. Parisi,[1,2] D. Geisler,[3] G. Carraro,[4] S. Villanova,[3] J. J. Clariá,[1,2] E. Costa,[5] M. Oddone,[1] N. Marcionni,[6] A. Grocholski,[7] A. Sarajedini,[7] and R. Leiton[3]

[1] *Observatorio Astronómico de Córdoba, Argentina*

[2] *CONICET, Argentina*

[3] *Universidad de Concepción, Chile*

[4] *European Southern Observatory, Chile*

[5] *Universidad de Chile, Chile*

[6] *Facultad de Matemática, Astronomía y Física, Argentina*

[7] *University of Florida, USA*

Abstract. We present metallicities for 15 Small Magellanic Cloud (SMC) star clusters. We add to this sample the ages and metallicities of 15 additional star clusters previously studied by Parisi et al. (2009) and Parisi et al. (2013), which were observed and analyzed following the same procedures as in the present work. Therefore, we compiled a sample of 30 SMC star clusters homogeneously studied, the largest sample to date. Metallicities are determined from the Calcium II triplet lines (CaT) in spectra obtained using the FORS2 multi-object spectrograph on the VLT (Paranal, Chile). Ages are determined from color-magnitude diagrams built from photometry of the pre-images. Using this sample, we analyze the chemical properties of the SMC, particularly the age-metallicity relation. We found three new old clusters which help to fill the so called SMC "age gap" between L 1 and NGC 121, the 2 oldest previously known clusters. These new old SMC clusters broadly increase our knowledge of the chemical evolution of this galaxy during the earliest epochs.

1. Observations

Using the FORS2 instrument on the Very Large Telescope (VLT, located on Paranal, Chile), we have obtained near infrared spectra for more than 500 red giant stars belonging to 15 clusters of the SMC and their surrounding fields. Spectra have a dispersion of ~ 0.85 Å/pixel, which is equivalent to a resolution of 2-3 Å, and cover a spectral range of ~ 1600 Å in the region of the three CaII lines. The observed clusters were located on the master CCD, while the observation of surrounding field stars was made using both the master and the secondary CCDs.

On the other hand, it was first necessary to obtain pre-images in the V and I bands for the selection of the spectroscopic targets. For that purpose, we requested the pre-

images to be taken with exposure times larger than usual, with the aim of obtaining relatively deep color-magnitude diagrams (CMDs) reaching well below the main sequence turn-off (MSTO) appropriate for cluster age derivation.

2. Age and Metallicity Determination

For each spectroscopically observed star, we measured radial velocities (RVs) and the equivalent width of the three CaT lines, following the same reduction and analysis procedures as in previous studies (Grocholski et al. 2006; Parisi et al. 2009). RVs were derived by performing cross-correlations between observed spectra and the spectra of 32 bright Milky Way open and globular template giants, which were defined by Cole et al. (2004). Equivalent widths were measured fitting a Gaussian+Lorentzian function to each CaT line. We then used the sum of the three CaT lines measured in each spectrum and the calibration of Cole et al. (2004) to derive the metallicity of each red giant. Cluster members were selected from an analysis which took into account not only the position of each star in the cluster and the CMD, but also its RV and metallicity. We calculated mean cluster metallicities only from those stars found to be cluster members. This article will only discuss the metallicities of the clusters, while the metallicity of the surrounding field stars will be discussed in a future work.

In the present analysis for our 15 clusters, we adopted ages reported in the literature, although we are in the process of making our own age determinations. For this purpose, we will perform PSF photometry on the V and I pre-images and we will build the corresponding CMDs. We then will measure the parameter δV, defined as the difference between the V magnitude of the clump and the MSTO. The parameter δV will be used together with the calibration of Carraro & Chiosi (1994) to derive cluster ages.

3. Sample Enlargement

In order to study global effects and to obtain better statistical errors, it would be good to have as large of a cluster sample as possible. In Parisi et al. (2009, hereafter P09), we derived the metallicities of another 15 SMC clusters following the procedures described in the previous section. Since the observation of these clusters was performed using the same telescope, instrument, and instrumental configuration as in the present work, we decided to add these clusters to the sample studied here. Thus, we have now a total of 30 SMC clusters with metallicities derived on a homogeneous scale. This enlarged sample is, at present, the largest and most accurate available cluster sample for the SMC. Moreover, in Parisi et al. (2013, hereafter P13) we derived the ages of the clusters studied in P09 by applying the procedure briefly described in Section 1.

4. Analysis

We show in Figure 1 (left panel) the metallicity distribution (MD) of the total SMC cluster sample. As can be seen, there is a suggestion of bimodality in the MD with possible peaks at ~ -1.05 dex and -0.77 dex. However, we calculated the statistical significance of a single vs. a double Gaussian fit and found that a two Gaussian fit does not turn out to be significantly better. The age distribution (AD, Figure 1 right panel)

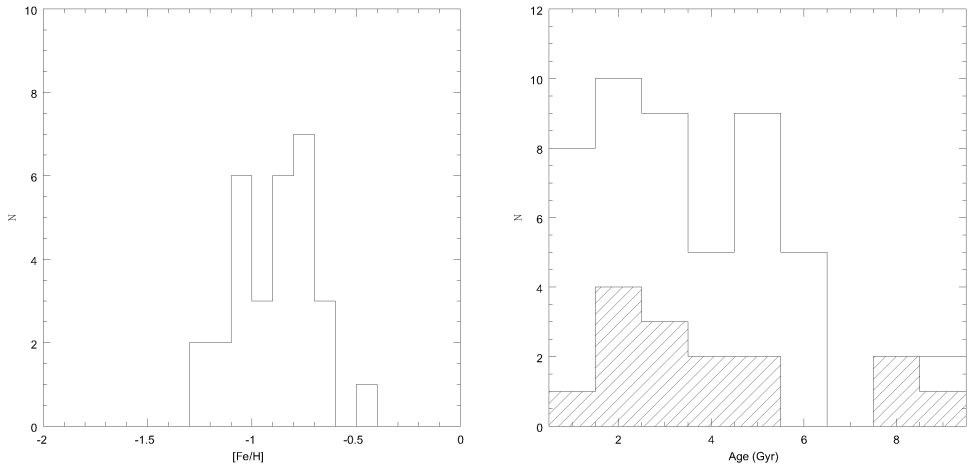

Figure 1. Left panel: Metallicity distribution of 30 SMC clusters, 15 of them from the present study and 15 from P09. Right panel: The SMC age distribution where the lined histogram represents the 15 clusters from P13, and the empty histogram represents 5 clusters from Piatti et al. (2001), 2 clusters from Piatti et al. (2007), 9 clusters from Piatti (2011a), 7 clusters from Piatti et al. (2011), 11 clusters from Piatti (2011b), 1 cluster from (Piatti 2012 and P13) and 15 clusters from P13.

obtained for our first 15 cluster sample studied in P13 reproduces the peak found by Piatti et al. (2011) at ∼ 2 Gyr, but it shows neither the second peak at ∼ 5 Gyr nor evidence of a constant formation rate as we move towards older ages. Because our cluster sample is statistically too small, we decided to enlarge it by adding 35 clusters studied using Washington photometry by Piatti et al. (2001, 2007); Piatti (2011a); Piatti et al. (2011); Piatti (2011b, 2012). The AD of this combined sample of 50 clusters reproduces the two peaks found in Piatti et al. (2011) at ∼ 2 Gyr and ∼ 5 Gyr (corresponding to possible episodes of cluster formation), but it does not show the formation rate found by them for the first ∼ 4 Gyr. The peak at 5 Gyr is in reasonable agreement with that in the field star formation rate at about 4.5 Gyr recently found in the study of Weisz et al. (2013). The second peak at ∼ 9 Gyr is not found in our data. However, this may be due to the statistically small number of clusters considered.

The age-metallicity relation (AMR) of our SMC cluster sample is shown in Figure 2. Circles represent our previously studied clusters for which we derived their CaT metallicities and ages in P09 and P13, respectively. Triangles represent clusters studied in the current research, whose ages were taken from the literature. We compare the observations with different models. The short dashed line in Figure 2 represents the model of closed box continuous star formation computed by Da Costa & Hatzidimitriou (1998); the solid line corresponds to the bursting model of Pagel & Tautvaisiene (1998), and the long dashed lined shows the infall-outflow model from field stars derived by Carrera (2005). While there seems to be a reasonable agreement between our observations and the bursting model for clusters younger than 3 Gyr, two important aspects are evident from Figure 2: (1) none of the currently available models completely reproduces the global behavior of the AMR, and (2) it is likely that there is not a unique AMR in the SMC. At any point, it is noticeable that there is a metallicity dispersion of ∼0.5 dex, which is considerably larger than the associated metallicity errors. It is

important to note that the metallicities presented in Figure 2 are homogeneous, in the sense that all clusters have been observed and analyzed following the same procedures.

We also calculated the mean metallicity of the clusters in different age bins and compared these values with those derived by Carrera et al. (2008) for field stars. Note that Carrera et al. (2008) derived the metallicity of field red giant stars using also the CaT technique. Figure 3 shows this comparison, wherein circles and squares represent ours and Carrera et al. (2008)'s mean values, respectively. As can be seen in Figure 3, clusters and field stars appear, on average, to have experienced the same chemical evolution. However, it is necessary to keep in mind the large metallicity dispersion exhibited in both clusters and field stars (see error bars in Figure 3).

5. New Old SMC Clusters

Using the age calibration of Carraro & Chiosi (1994), we found that three clusters of our sample, L 110, L 4 and L 6, are newly discovered to be very old SMC clusters (t = 7.61 ± 1.03, 7.93 ± 1.07 and 8.7 ± 1.18 Gyr, respectively). Thus, we have significantly enlarged the number of currently known old clusters in the SMC.

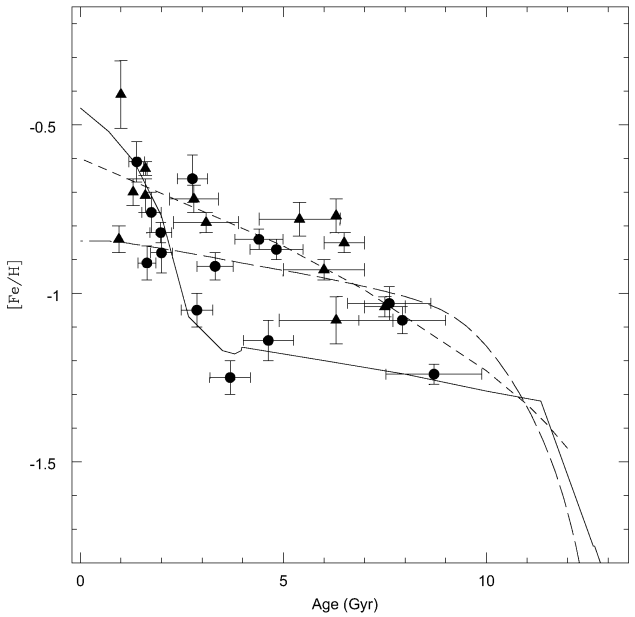

Figure 2. The age-metallicity relation of our SMC cluster sample is shown. Circles represent clusters previously studied, for which we have derived their CaT metallicities and ages in P09 and P13, respectively. Triangles are our new cluster sample where we have taken their ages from the literature. The short dashed line represents the model of closed box continuous star formation computed by Da Costa & Hatzidimitriou (1998). The solid line corresponds to the bursting model of Pagel & Tautvaisiene (1998), while the long dashed line shows the best-fit model derived by Carrera (2005).

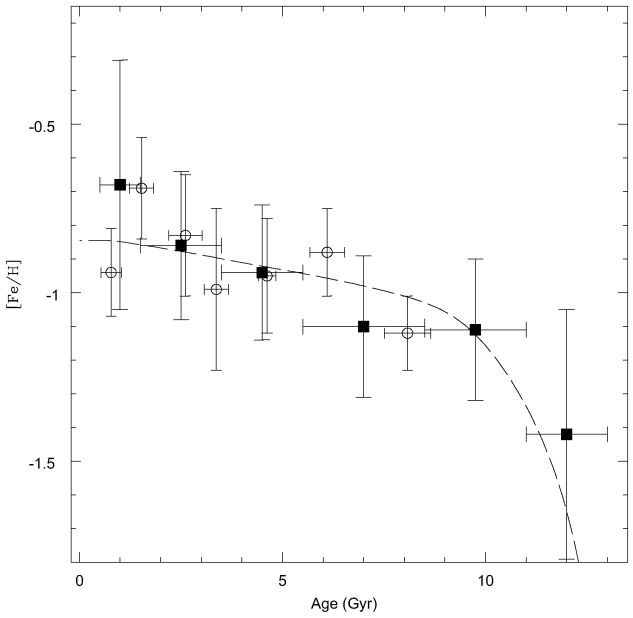

Figure 3. The mean CaT metallicity in different age bins is shown for the clusters (circles, P09 and present work) and field stars (squares, Carrera et al. 2008). The curve corresponds to the best fit chemical evolution model for field stars (Carrera 2005).

In order to corroborate the old nature of our three new old clusters, we derived their ages by applying two independent methods. First, we derived a new calibration (SMC

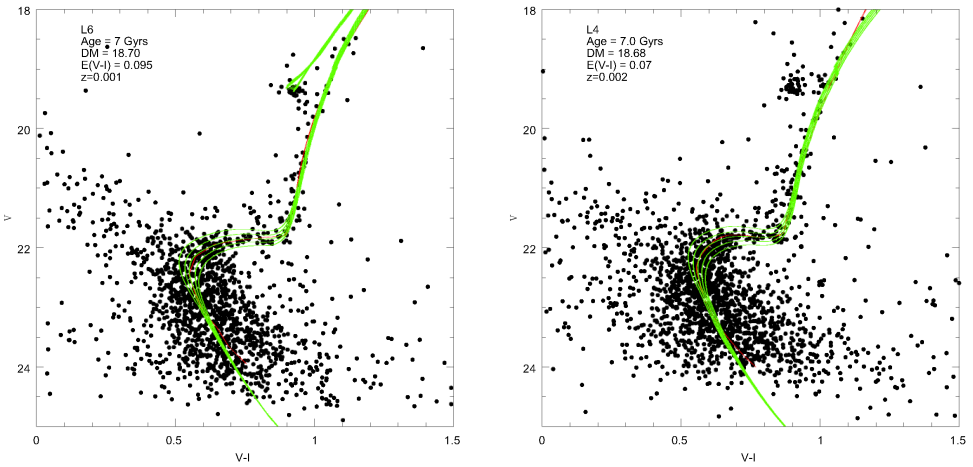

Figure 4. *Left panel:* The CMD of L 6 is presented. We show Teramo isochrones as solid lines (colored green in the online version). They cover an age range from 6 to 8 Gyrs in steps of 0.5 Gyrs. The central isochrone, which best reproduces the fiducial ridgeline (red line in the online version), is the one that we have adopted. Fitting parameters are listed in the plot. *Right panel:* Same as left panel but for the cluster L 4 and using Dartmouth isochrones in age steps of 6, 6.5, 7, 7.5 and 8 Gyrs.

δ calibration) using the SMC clusters studied by Glatt et al. (2008a,b) with the HST. Our new calibration is valid for clusters older than $\sim$ 6 Gyr with similar metallicities ([Fe/H] ~ -1dex). Using the SMC δ calibration, we found that L 110, L 4 and L 6 are 6.62, 6.94 and 7.67 Gyr old, respectively. According to this procedure, all three clusters are about the same age as L 1 at 7.5 Gyr, with L 6 being slightly older, and L 4 and L 110 a bit older than the next oldest clusters in the Glatt et al. sample at 6.5 Gyr. Secondly, we calibrated our VLT photometry with independent observations and we fitted different set of isochrones to the calibrated CMDs, confirming the old nature of these three clusters: Padova (Girardi et al. 2000), Teramo (Pietrinferni et al. 2004) and Dartmouth isochrones (Dotter et al. 2007). We show in Figure 4 examples of isochrone fits for clusters L 4 and L 6.

References

Carraro, G., & Chiosi, C. 1994, A&A, 287, 761

Carrera, R. 2005, Ph. D. Thesis, Departamento de Astrofísica, Universidad de La Laguna, España.

Carrera, R., Gallart, C., Aparicio, A., Costa, E., Méndez, R. A., & Noël, N. E. D. 2008, AJ, 136, 1039

Cole, A. A., Smecker-Hane, T. A., Tolstoy, E., Bosler, T. L., & Gallagher, J. S. 2004, MNRAS, 347, 367

Da Costa, G. S., & Hatzidimitriou, D. 1998, AJ, 115, 1934

Dotter, A., Chaboyer, B., Jevremović, D., Baron, E., Ferguson, J. W., Sarajedini, A., & Anderson, J. 2007, AJ, 134, 376

Girardi, L., Bressan, A., Bertelli, G., & Chiosi, C. 2000, A&AS, 141, 371

Glatt, K., Gallagher, J. S., III, Grebel, E. K., Nota, A., Sabbi, E., Sirianni, M., Clementini, G., Tosi, M., Harbeck, D., Koch, A., & Cracraft, M. 2008a, AJ, 135, 1106

Glatt, K., Grebel, E. K., Sabbi, E., Gallagher, J. S., III, Nota, A., Sirianni, M., Clementini, G., Tosi, M., Harbeck, D., Koch, A., Kayser, A., & Da Costa, G. 2008b, AJ, 136, 1703

Grocholski, A. J., Cole, A. A., Sarajedini, A., Geisler, D., & Smith, V. V. 2006, AJ, 132, 1630

Pagel, B. E. J., & Tautvaisiene, G. 1998, MNRAS, 299, 535

Parisi, M. C., Geisler, D., Carraro, G., Clariá, J. J., Costa, E., Grocholski, A. J., Sarajedini, R., A. Leiton, & Piatti, A. E. 2013, AJ, submitted

Parisi, M. C., Grocholski, A. J., Geisler, D., Sarajedini, A., & Clariá, J. J. 2009, AJ, 138, 517

Piatti, A. E. 2011a, MNRAS, 416, L89

— 2011b, MNRAS, 418, L69

— 2012, ApJ, 756, L32

Piatti, A. E., Clariá, J. J., Bica, E., Geisler, D., Ahumada, A. V., & Girardi, L. 2011, MNRAS, 417, 1559

Piatti, A. E., Santos, J. F. C., Clariá, J. J., Bica, E., Sarajedini, A., & Geisler, D. 2001, MNRAS, 325, 792

Piatti, A. E., Sarajedini, A., Geisler, D., Gallart, C., & Wischnjewsky, M. 2007, MNRAS, 381, L84

Pietrinferni, A., Cassisi, S., Salaris, M., & Castelli, F. 2004, ApJ, 612, 168

Weisz, D. R., Dolphin, A. E., Skillman, E. D., Holtzman, J., Dalcanton, J. J., Cole, A. A., & Neary, K. 2013, MNRAS, 431, 364